

Internal length and time scales in a simple shear granular flow

Hayley H. Shen* and Balasubramanian Sankaran

Department of Civil and Environmental Engineering, Clarkson University, Potsdam, New York 13699-5710, USA

(Received 16 November 2003; revised manuscript received 9 February 2004; published 16 November 2004)

Kinetic theory has been successfully applied to mathematically model the constitutive relations for flowing granular materials. However, the basis for kinetic theory is the assumption of binary collisions between particles. Both physical and numerical experiments of granular flows have questioned the validity of this assumption. It is known that when solid concentration or shear-rate increase, collision contact time becomes long relative to free-flight duration. Multiple collisions begin to prevail. Interactions between groups of particles may dominate the dynamics of the flow. This paper addresses both the size and lifetime of multiple collision groups in a granular flow. Computer simulations of a simple shear two-dimensional assembly of visco-elastic particles with or without friction are performed. It is found that as the shear-rate or solid concentration increase the shearing particles begin to form distinct groups within each group particles collide simultaneously. The group size grows with further increase of shear-rate or solid concentration to the extent that force chains spanning the whole shearing assembly may form. Concomitantly the collision duration also increases far beyond that of a binary collision. The evolution of the group size and the collision duration are associated with the change of the constitutive behavior of the granular materials. The existence of additional length and time scales demands new formulation for granular flows.

DOI: 10.1103/PhysRevE.70.051308

PACS number(s): 45.70.-n

I. INTRODUCTION

Theories of constitutive relations for rapidly flowing granular materials are mainly based on extensions of the kinetic theory of gases [1]. A review of this development may be found in Ref. [2]. These theories assume that the collision time is negligible compared to the mean free flight time of the particles. Therefore stresses are generated solely from binary collisions. Such an assumption is valid in case of dilute granular flows. However most of the granular flows are dense in nature. Particle interactions can involve multiple grains and interaction time can be significantly longer than the binary collision duration. The size of multiple grains and the long particle interaction time alter the rheology of granular flows.

The formation of clusters in a rapidly sheared granular flow has been observed in computer simulations even at moderate solid concentrations [3,4]. These structures are more pronounced in highly dissipative systems. Relaxation behavior of these structures is called “granular cooling” [5,6]. Although clusters only mean enhanced proximity of neighboring particles not necessarily in simultaneous contact, the existence of clusters indicates high local concentration, which suggests the possibility of multiple collisions among neighboring particles. The immediate implication of multiple collisions is the additional length scale associated with the size of the simultaneously contacting particles, and the additional time scale associated with the duration of collisional contacts.

In this paper we simultaneously introduce an internal length parameter: the “group size” and a time parameter: the “contact lifespan.” The “group size” is defined as the number

of interconnecting particles by contact. A “group” is thus different from a “cluster” referred in [3,4] in that all particles of the same group must be interconnected by mutual contacts. The “contact lifespan” is defined as the duration of a collision. The effects of shear-rate and solid concentration on these internal length and time scales are investigated by using a computer simulation of two-dimensional simple shear flow of viscoelastic disk assemblies with or without interparticle friction.

II. BACKGROUND OF THE PROBLEM

The stress in a granular system consists of two parts—contact stress and kinetic stress, the latter is also called the streaming stress [7,2]. The kinetic part comes from particle fluctuations about the mean velocity and the contact part is from the force between colliding particles. The contact part dominates the total stress unless the solid concentration is very low [8]. The underlying concept of the kinetic theory of granular materials is that collisions produce linear momentum transfer. The rate of momentum transfer results in stresses. Hence stresses are expected to be proportional to the product of collision frequency and the momentum transfer in each collision. The frequency of collision and momentum transfer in each collision are both proportional to the relative velocity of neighboring particles, and such relative velocity is proportional to the shear-rate in a simple shear situation, thus the collisional stress ought to be proportional to the square of the shear-rate in this type of flows.

From a computer simulation of a simple shear flow of uniform disks, it was found that the stress and shear-rate relation did not always follow the rate dependency described above [9]. As the solid concentration increased keeping all other parameters constant, the stress changed from a quadratic dependence on the strain-rate to nearly independent of

*Email address: hhshen@clarkson.edu

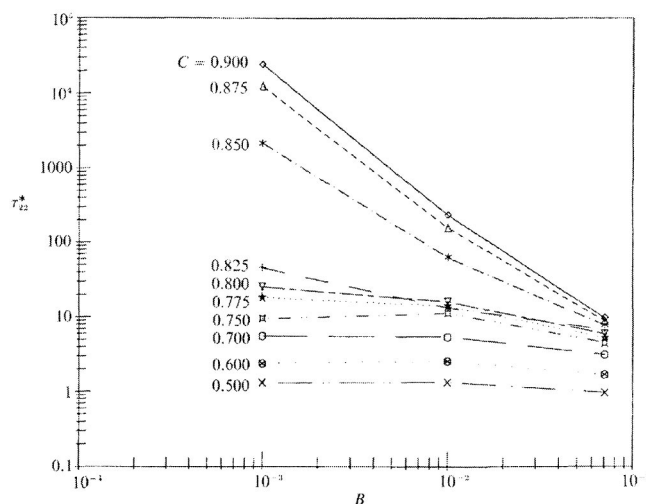


FIG. 1. Dimensionless normal stress vs dimensionless shear-rate B at various solid concentrations C (from Ref. [9]).

the strain-rate. Figure 1 shows this phenomenon.

In the figure, $\tau_{22}^* = \tau_{22} / \rho_s D^2 \dot{\gamma}^2$ is the dimensionless normal stress, $B = \dot{\gamma} / \sqrt{K_n / \rho_s (\pi/4) D^2}$ is the dimensionless shear-rate, where $\dot{\gamma}$ represents the shear-rate, D the particle diameter, ρ_s its unit thickness density, K_n spring stiffness in the normal direction, and C solid concentration. At a high solid concentration ($C=0.9$) the slope of the curve is approximately -2 , indicating that the dimensional stress τ is independent of shear-rate. At a low concentration ($C=0.5$) the slope of the dimensionless stress becomes flat, indicating that the dimensional stress is proportional to the square of the shear-rate. The degree of rate dependency varies between these two extremes for intermediate concentrations. This finding led to a regime theory proposed in Ref. [9]. A schematic flow map was given in terms of concentration and dimensionless shear-rate. The coordination number was suggested as the possible internal parameter that could control the change of rate dependency.

More data supporting the same phenomenon as shown in Fig. 1 were obtained in a recent three-dimensional study of spheres [10]. In which, the regime change was further derived from a range of friction, concentration, and the dimensionless shear-rate. Detailed flow map was obtained from a large set of computer simulation data, supporting the schematic regime chart proposed in Ref. [9]. The importance of friction coefficient was discussed as it controlled the strength of the force chains that formed inside the granular flow at high concentrations. Duration of contact time was linked to multiple particle collisions.

Many authors questioned the validity of binary collisions in high solid concentration from the inception of the rapid granular flow theory. Heuristic modifications to the constitutive relations have been proposed [11–13]. In order to bridge the “kinetic” type of behavior where stresses depend on the shear-rate to “quasistatic” type where stresses are independent of shear-rate, these authors proposed constitutive laws that linearly combined both rate-dependent and rate-independent stress contributions. While functionally satisfactory as they are for simple cases such as flow down an in-

cline, a fundamental understanding of the transition between “kinetic” and “quasistatic” granular behaviors is needed.

A review article summarized many recent physical and numerical studies of the “granular gases,” i.e., the rate-dependent granular flows [14]. The existence of internal structures and inseparable time scales were discussed, in which the structures were associated with clusters (or density inhomogeneities as discussed in Refs. [3,4]) or correlation lengths. Another well-recognized internal structure discussed was the load-bearing force chains that exist in quasistatic rate-independent granular flows, as observed experimentally with photoelastic materials [15–17]. The dynamics of formation and collapse of the force chains also present length and time scales.

Intuitively these internal structures and additional length and time scales must play a role in the constitutive relations for granular flows. Quantitative theories that implement these parameters await development.

In a recent study [18], a detailed analysis of probabilistic distribution of contact duration and its effect on constitutive relations was given. A time scale relating to the contact “age” in granular shear flows was proposed. It was found that in dense granular flows most of the collisions lasted much longer than the binary collision duration. A theoretical argument for the “age” distribution of collision contacts was provided, and a new time scale was introduced. By using this new “relaxation time” of multiple collisions a viscoplastic constitutive law for granular flows was obtained that smoothly bridged the fluid-to-solid transition.

Meanwhile, studies concentrating on the spatial structures have also been actively pursued recently. For instance, Ref. [19] studied the transition between “fluid-like” and “solid-like” shearing behavior in a wall-bounded flow with fixed wall pressure. Where “fluid-like” referred to shearing in a boundary layer next to the moving wall and “solid-like” referred to interior shear similar to failure zones developed in collapsed soil. In “fluid-like” cases the force chains were predominantly linear, while in “solid-like” cases the force chains formed a network consisting two nearly perpendicular directions. Ref. [20] investigated a constant pressure, thin Couette cell numerically and decomposed the total stress into “fluid contact” stress and “solid contact” stress. Only those forces from nonsliding contacts that last longer than binary collision contribute to “solid stress.” An “order” parameter determined by the changes in the contact fabric was introduced. A constitutive law is proposed that relates stresses to this order parameter.

Clearly with the rapid increase of studies trying to relate constitutive behavior of granular flows to the internal structures, both spatial and temporal, new insights are mounting fast. In the next section we propose a conceptual theory that attempts to describe the evolution of constitutive behavior of granular flows from dilute to dense concentration that covers low to high shear rates. In addition to the contact duration, we will introduce a new length scale called “group size” defined by the number of simultaneously colliding particles. The new length scale is the central idea of this conceptual theory. The relation of this length scale and the associated contact duration with the concentration, shear-rate, and material properties of the granular assembly will be investigated.

III. A CONCEPTUAL THEORY

In this section we will provide a possible physical explanation for the evolution of granular shear flows from a rate-dependent regime to a rate-independent regime. Consider a dry granular flow, the essential parameters that determine the constitutive relations are

$$\tau = F(\dot{\gamma}, D, \rho_s, \mu, K, e, C). \quad (1)$$

In the above, the additional parameters not defined earlier are μ frictional coefficient, K spring constant (normal or tangential), and e coefficient of restitution in particle-particle collisions. There are several ways to obtain the dimensionless form of the above equation, depending on how the stress is nondimensionalized. Let m be the particle mass, the two below are both valid dimensionless forms:

$$\frac{\tau}{\rho_s D^2 \dot{\gamma}^2} = F_1\left(\frac{\dot{\gamma}}{\sqrt{K/m}}, \mu_s, e, C\right) \quad (2a)$$

or

$$\frac{\tau D}{K} = F_2\left(\frac{\dot{\gamma}}{\sqrt{K/m}}, \mu_s, e, C\right). \quad (2b)$$

The left is the one presented in Fig. 1. As discussed in [18], in the collisional regime particle stiffness is irrelevant and stress is strongly rate-dependent, thus Eq. (2a) is more appropriate for characterizing the constitutive relation. In the quasistatic regime particle stiffness dominates while shear-rate becomes irrelevant and Eq. (2b) is more appropriate.

There are two obvious time scales in granular shear flows [9,10]. One is the duration of a binary collision t_c and the other is the free flight time t_f . In the following, we will briefly reiterate the consequence of these two time scales.

If we assume a linear spring and dashpot contact mechanics such as most of the rapid granular studies have adopted, the contact duration may be solved in terms of the restitution coefficient. As shown in [9,10], the duration of contact is $t_c = \pi / \sqrt{(2K/m)(1-\zeta^2)}$ where $\zeta = -\ln e / \sqrt{\pi^2 + \ln^2 e}$ is the damping coefficient associated with the dashpot. Hence

$$t_c \propto \sqrt{\frac{m}{K(1-\zeta^2)}}. \quad (3)$$

The true free flight duration is a function of the particle velocity and the mean free path. The particle velocity is consisted of both the mean velocity and the particle's fluctuation. Using an order of magnitude argument, both mean relative velocity between particles and particle's fluctuation velocity are proportional to the shear-rate times the particle diameter. The separation between particles is proportional to their diameters for a fixed concentration. We thus estimate $t_f \propto \dot{\gamma}^{-1}$ with the proportionality strongly dependent on concentration.

If the duration of binary collision is much shorter than free flight, binary collision would be the dominant mode of stress generation, and constitutive laws derived from the kinetic theory apply [1]. In dimensionless form, the relative magnitude of binary collision duration to the free flight duration gives the ratio

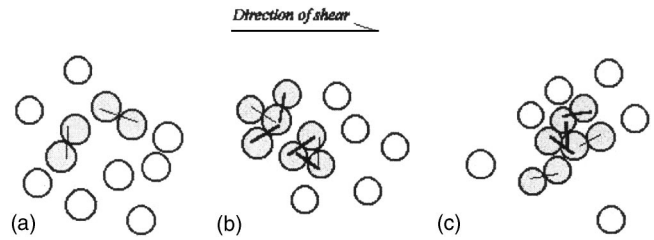


FIG. 2. Low concentration. (a) Very low shear-rate; (b) intermediate shear-rate; (c) high shear-rate.

$$\frac{t_c}{t_f} \propto \dot{\gamma} \sqrt{\frac{m}{K(1-\zeta^2)}} = \frac{B}{\sqrt{1-\zeta^2}}, \quad (4)$$

where $B = \dot{\gamma} \sqrt{m/K}$ is the dimensionless shear-rate and m is the particle mass. For any fixed damping effect ζ , low shear-rate means $B \ll 1$, which implies $t_c \ll t_f$. In this case we may apply the kinetic theory and the flow approaches the theoretical ‘‘rapid’’ flow. On the other hand, high shear-rate means $B \gg 1$ and $t_c \gg t_f$ which implies multiple collisions, group formation, and eventually force chain development.

As mentioned in Refs. [9,10] the above observation seemed to contradict the common notion that ‘‘rapid’’ flow is synonymous to fast flow. The former implies the kinetic theory and the latter implies high shear-rate. This paradox is actually easily resolved when we consider the conventional shear tests, in which indeed high shear-rates lead to stresses that are proportional to the square of the shear-rate [21,22]. These tests are conducted with a fixed normal stress. In granular flows, shearing generates a dispersive normal stress. When the confining normal stress is fixed, as the shear-rate increases the granular material must dilate. Hence the solid concentration decreases, free flight time increases, and the flow becomes more inertia-dominant where kinetic theory applies.

To gain realistic appreciation of the time scales, we consider a case of sand grains. For Young's modulus of the order of 100 MPa, and grain size of 1 mm in diameter, the binary contact time estimated with Eq. (3) is of the order of 10^{-5} sec. With this in mind it would seem that for the free flight time scale to be comparable with the duration of a binary collision the shear rate is unattainably high. However, the free flight time scale t_f is highly sensitive to the solid concentration, because the average distance between grains is proportional to $\sqrt{C_0/C} - 1$ in 2D and $\sqrt[3]{C_0/C} - 1$ in 3D, where C_0 is the densely packed concentration. Therefore, as

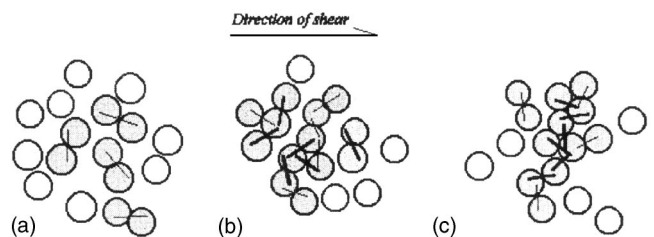


FIG. 3. Intermediate concentration. (a) Very low shear-rate; (b) intermediate shear-rate; (c) high shear-rate.

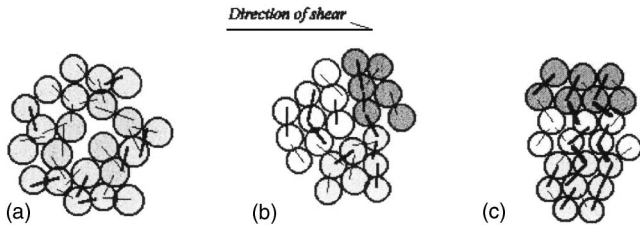


FIG. 4. High concentration. (a) Very low shear-rate; (b) intermediate shear-rate; (c) high shear-rate.

the concentration increases, free flight time drastically reduces and multiple collisions will prevail.

As shown in Ref. [18], in addition to the two time scales described above another time scale associated with the relaxation of multiple collision groups emerges. This time scale depends on the existing intrinsic parameters of the granular assembly. It is very likely that many other secondary time scales will prove to be important as the granular flow evolves from inertia-dominant to quasistatic.

What exactly happens inside a granular material when it goes through the transition? From physical experiments [23] and computer simulations [24], it is clear that internal particle organization evolves when solid concentration is high. In our conceptual model, the transition from inertia-dominant to quasistatic flow is a result of the internal structure evolution. We will describe this evolution pictorially by considering three cases: a low, an intermediate, and a high concentration case.

In each of the three cases, the materials are the same. Let us begin with the low concentration case, as shown in Fig. 2. This figure shows a scenario of increasing shear-rate from left to right while keeping the concentration constant. Shaded particles are in contact. At a very low shear-rate as in Fig. 2(a), the shear-induced particle velocity is low. Hence the travel time between collisions is longer than the contact time between colliding particles. Binary collisions prevail. Contact forces (the equal and opposite pair) between colliding particles are shown as bars connecting particles. Each contact force consists of a normal and a tangential component. The thickness of the force bars represents the magnitude of the combined force and the direction of the combined force is the direction of the bar. As the shear-rate increases, the traveling time between collisions reduces and the probability of multiple collisions goes up. As shown in Fig. 2(b), two groups of three or four particles are engaged in multiple collisions. These particle groups disperse shortly after and new groups form. When shear-rate is further increased as in Fig.

2(c), groups grow in size due to an increasing chance for free particles to join before groups have the time to disperse. Conceivably, there may be a maximum group size depending on the global concentration, the shear-rate, and material properties. As the solid concentration approaches zero, the group size should approach one. The maximum possible group size under any condition is the total number of particles in the flow domain.

Next we consider an intermediate concentration case. Figure 3 depicts a scenario from a very low shear-rate to increasingly higher and higher shear-rates. At very low shear-rates, binary collisions still have a chance to finish before a traveling particle comes along to begin the next binary collision, as in Fig. 3(a). As the shear-rate increases, just like in Fig. 2, multiple collisions become increasingly probable. At this intermediate concentration, however, the number and size of groups are greater than the low concentration case. Furthermore, as the shear-rate increases more, large groups that span the entire length of the granular assembly in the shear gradient direction can form, such as in Fig. 3(c). At this intermediate concentration, these large groups, or force chains, are short-lived. They dynamically deform and break-down into smaller groups and reform into new force chains.

At a high concentration as shown in Fig. 4, almost all particles are connected all the time through a force network. When shear-rate is very low, such as in Fig. 4(a), particles have time to rearrange, so that groups may move over one another to accomplish a macroscopic shear-rate. This concept is analogous to that of the liquid viscosity [25]. As the shear-rate increases, the time to rearrange cannot catch up, particles form crystallized regions joined by slip-lines. Figure 4(b) shows such a case, where different particle shadings represent different groups bordered by slip-lines. These crystallized groups maintain their identity much longer than those in Fig. 4(a). These groups slide across one another as well as undergo deformation within the individual groups. The slip-lines rotate gradually as the crystallized groups slide and deform. A time sequence of such phenomenon is shown in Fig. 5. As the shear-rate increases even more, the only way shear can happen is through formations of concentrated failure zones. The white particles in the center two layers of Fig. 4(c) represent this failure zone, most of the shear takes place in this failure zone, the rest of the particles remain crystallized, with no time to relax and rearrange. This stage also represents very high peak stress levels. Particles may fracture under the peak contact load. Formation of such localized shearing layer in granular flows was found in [9,10]. The transition between Figs. 4(b) and 4(c) is analogous to ductile/brittle transition in solids.

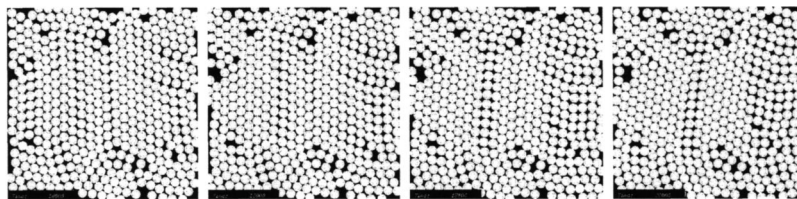


FIG. 5. A time sequence of deforming blocks of granular materials joined by slip-lines. $C=0.875$; $\mu=0.5$; $e=0.1$; $B=0.001$; sample size=30 (in flow direction) by 100 (in velocity gradient direction). Velocity is in the horizontal direction and gradient is in the vertical direction. These panels are separated by a time duration of $10t_c$.

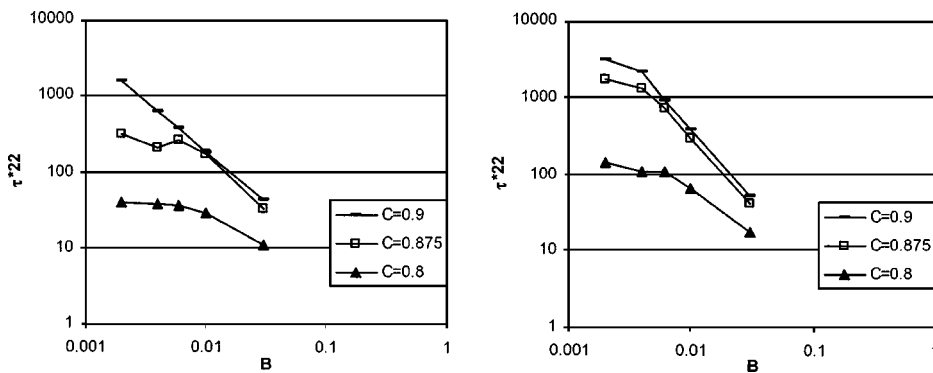


FIG. 6. Dimensionless normal stress vs dimensionless shear-rate B . Left side: $\mu=0$; right side: $\mu=0.5$.

In dimensionless terms, “low shear-rate” corresponds to $t_c/t_f \ll 1$, “high shear-rate” corresponds to $t_c/t_f \gg 1$ and “intermediate shear-rate” is the case $t_c/t_f \approx 1$. Because the ratio of binary contact duration and the mean free flight time approaches infinity as the solid concentration approaches the densest packing, at extremely high concentration close to the maximum packing limit, it is conceivable that situations depicted in Figs. 4(a) and 4(b) are impossible. As soon as the shear begins, the particles form crystallize regions and shear can only occur at finite failure zones. In this case, the condition we call “high shear-rate” as shown in Fig. 4(c) can begin at a physically very low value of shear-rate. Stick-slip situation at very high concentrations has been observed in several physical and computational studies of granular materials (e.g., Ref. [26]). That is, shearing occurs discontinuously in time and a constant shear-rate cannot be maintained. This situation is not covered by Fig. 4(c). We believe that Fig. 4(c) is only one kind of flow that happens under high concentration and “high” shear-rate. The formation of a failure zone is necessary to allow a continuous shear at a constant rate. This failure zone is most likely created by first applying a slow strain such as in a triaxial test vessel. If a granular material does not have the time to create this failure zone, it must then go through an elastically deforming stage (stick) until enough room is created somewhere so that a local collapse takes place, and shear can be accomplished (slip), provided that particles survive the high deformation stage.

It should be emphasized that although there are nine distinct “regimes” depicted in Figs. 2–4, transition between any pairs of these regimes may be gradual or abrupt. Indeed, from the flow maps shown in [10], the transition between some basic regimes defined as elastic-quasistatic, elastic-inertial, inertial-noncollisional, and inertial-collisional could occur over small changes in the parameter space.

IV. THE NUMERICAL EXPERIMENT

To validate the above conceptual theory, we performed a numerical experiment using the discrete element method as described in Ref. [9]. For completeness, this numerical model is briefly described here. A two-dimensional assembly of uniform disks is adopted. We consider a simple shear flow with velocity in the x direction and velocity gradient in the y direction. The contact force between two disks consists of normal and tangential components. A parallel linear spring

and dashpot is applied in the normal direction and a linear spring with frictional sliding is applied in the tangential direction. The spring and dashpot forces are directly related to the relative velocity between two particles A and B

$$\vec{V}_{AB} = (\dot{x}_A - \dot{x}_B) + R(\dot{\theta}_A + \dot{\theta}_B)\hat{t} \quad (5)$$

where \vec{x} is the position vector of the particle, R is particle radius, θ is the angular displacement of the particle, and \hat{t} is the unit vector tangent to the particles in contact. The relative displacement rates in the normal and tangential directions may be expressed as $\dot{n} = \vec{V}_{AB} \cdot \hat{k}$ and $\dot{q} = \vec{V}_{AB} \cdot \hat{t}$ respectively, in which, \hat{k} is the unit normal vector at contact. Using these notations, the damping forces due to dashpots are calculated in terms of the instantaneous relative velocity

$$D_n = 2\zeta_n \sqrt{mK_n \dot{n}}, \quad (6)$$

where K_n is the normal spring constants of contact and ζ_n is related to the restitution coefficient e as defined in Eq. (3).

The normal and shear spring forces are cumulated such that at time step N

$$F_n^N = F_n^{N-1} + K_n \dot{n}^{N-1/2} \Delta t \quad \text{and} \quad F_s^N = F_s^{N-1} + K_s \dot{q}^{N-1/2} \Delta t. \quad (7)$$

The total force is the sum of dashpot (damping) and spring forces defined above. The magnitude of the shear force is limited by μF_n where μ is the friction coefficient.

The material parameters used in the present simulations are spring constant in the normal direction $K_n = 10^6$, tangential directions $K_t = 0.8K_n$, particle diameter $D = 1$, and particle mass = 1. Two friction coefficients are studied: $\mu = 0$ and $\mu = 0.5$. When $\mu = 0$ slipping always occurs if there is any tangential relative momentum. Two values of restitution coefficient were investigated, $e = 0.1$ and $e = 0.9$, in the normal direction, and no damping in the tangential direction. In the figures to follow, we present the case when $e = 0.1$. The results are qualitatively the same for the case with $e = 0.9$.

Periodic boundary conditions are applied, which is a standard technique well established in molecular dynamics [27]. The number of simulation domain contains 3000 particles (30 in the velocity direction by 100 in the velocity gradient direction). In each time step, list of neighboring particles are first established through a search routine. Contacts are then detected if center-to-center distance between neighboring particles is less than a particle diameter. All contacts binary or multiple, are recorded first, then total contact force acting

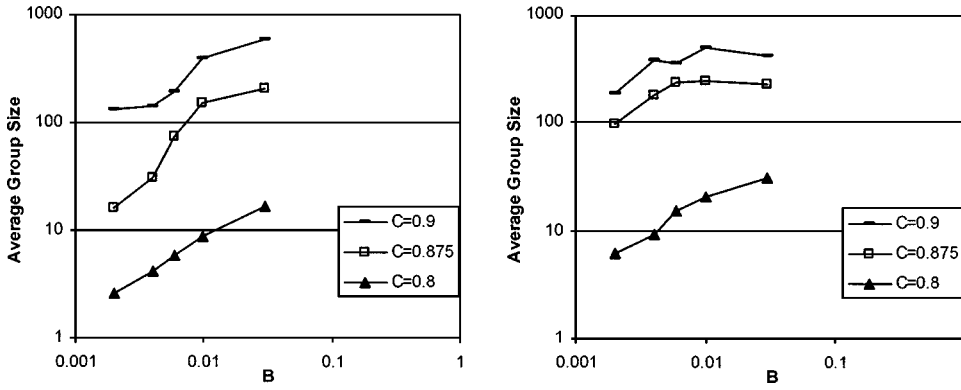


FIG. 7. Average group size vs dimensionless shear-rate B . Left side: $\mu=0$; right side: $\mu=0.5$.

on a particle is calculated from the sum of all individual contact. The acceleration, velocity, and displacement of each particle are obtained from the total force. The computation proceeds to the next time step.

The total stress is the sum of the kinetic stress τ^k and the contact stress τ^c . The contact stress is defined as $\tau_{ij}^c = \langle k_i F_j \rangle = (D/A) \sum_{c=1}^M k_i F_j$ where D is the disk diameter, A is the domain area, M is the number of contacts in A , k is the contact vector and F is the contact force between two disks. The kinetic stress is defined as $\tau_{ij}^k = -\langle \rho v_i^p v_j^p \rangle = -(m/A) \times \sum_{p=1}^N v_i^p v_j^p$ where $\rho = mN/A$ is the density of the particle assembly, m is the disk's mass, N is the particle number in the domain and v^p is the fluctuation velocity of the particles. The time step was chosen to be 1/50 of the binary collision time. All data reported here are based on steady state results as determined by the average stress levels.

Figure 6 shows the dimensionless stress obtained for three concentrations. Although the material properties are very different and sample size is 100 times of that reported in Ref. [9], similar variation of rate dependency as shown in Fig. 1 is again observed for both frictionless and frictional cases, with higher stresses in the latter case.

We define simultaneously contacting particles as a "group." These "groups" are somewhat like macroparticles except that they can deform, disintegrate, and reorganize. Two distinct groups do not have any particles in contact with each other, but all particles belonging to the same group are connected via force networks. In strictly binary collision cases, group size is either 1 for free flight particles or 2 for a pair in collision. Figure 7 is the result of the average group size, defined as the total number of particles divided by the number of groups in the simulation domain. In each case group size increases with increasing shear-rate, as expected

based on the conceptual theory described earlier. Except for one case at the highest concentration and highest shear rate, friction consistently increases the average group size. Figure 8 shows the maximum size of the groups. Since the total number of particles is 3000 in the numerical experiment, when the maximum size of the group reaches 3000, force chains spanning the entire domain are present and the system "saturates." For the frictionless case, this condition is reached when C is 0.9 and the dimensionless shear-rate is greater than 0.01. For the frictional case, force chains spanning the entire domain occur earlier, as seen from the much higher values of maximum group size in the entire range of shear rate studied. Force chains may develop much earlier than the moment when maximum group size equals the sample size. In fact, as soon as one group of simultaneously colliding particles spans the flow domain in any direction, force chain forms. However, we currently do not have any geometric measure of a group other than its size, hence we are not equipped to detect the onset of force chains spanning the domain.

The variation of coordination number with respect to the dimensionless shear-rate is shown in Fig. 9. Clearly, the coordination number increases with the concentration. But the dependence on the shear-rate is not monotonic. Coordination number is a measure of rigidity in polymer fluids and granular materials [28]. A degree of freedom constraint argument was used to suggest that for critical rigidity the coordination number is $z_c=4$ for stationary smooth uniform disks and $z_c=3$ for the corresponding situation with frictional disks. Below this critical number granular materials cannot support load from arbitrary directions. Figure 9 shows that for flowing granular materials, as the shear-rate increases, the coordination number approaches $z_c=3$ in different fashions depending on the concentration. For a very high concentration

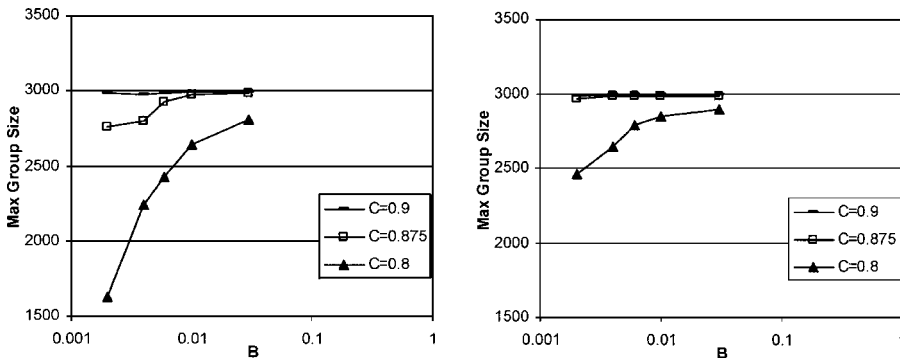


FIG. 8. Maximum group size vs dimensionless shear-rate B . Left side: $\mu=0$; right side: $\mu=0.5$.

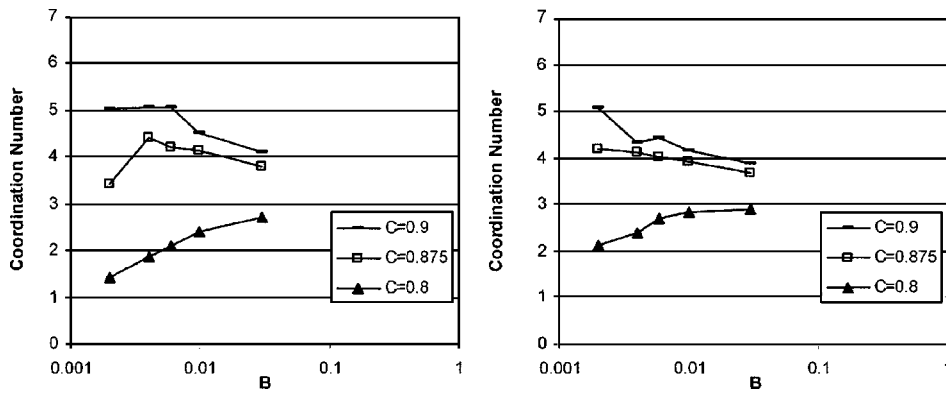


FIG. 9. Coordination number vs dimensionless shear-rate B . Left side: $\mu=0$; right side: $\mu=0.5$.

($C=0.875, 0.9$) the coordination number decreases to 3 as shear-rate increases. For a lower concentration ($C=0.8$) the coordination number increases to 3. This phenomenon is observed for both frictionless and frictional cases.

Figure 10 shows the contribution of the kinetic stresses to the total stresses. This contribution increases as the shear-rate increases. Increasing kinetic stress indicates higher particle velocity fluctuation, hence implies less stable particle groups. For the two cases of very high solid concentration ($C=0.875, 0.9$) fluctuation energy increases as the coordination number decreases. For the case of a lower concentration ($C=0.8$) increasing fluctuation does not affect the increase of the coordination number. The relation among fluctuation energy, coordination number, and the stability of groups will require further investigations.

To test the stability of groups we may also study the contact duration. Moreover, contact duration is a measure of the validity of kinetic theory. We define the contact duration as the duration from the initiation of a contact to its termination, that is, the “lifespan” of a collision. The measure of this duration is inherently limited by the observation. Contact durations longer than the observation duration can only be recorded as “saturated.” As shear-rate increases, it was observed that the contact duration also increases. Hence, it is necessary that the observation length be increased for large shear-rates or higher solid concentrations. In the results presented here, the time range for observing the contact duration of the particles is between 2000 and 4000 time steps, or 50 to 80 times the binary collision duration t_c . To obtain smooth statistics we bin the duration of contacts over a small range of time steps, the bin sizes are 40 for $C=0.8$, 60 for $C=0.875$, and 80 for $C=0.9$.

Figure 11 shows the number density of the dimensionless contact duration for $\mu=0$, three concentrations and two shear-rates. If all contacts are binary, the number density function should have a delta distribution around 1. As can be seen, for lower shear-rates, contact durations are closer to that predicted by the binary collision duration than higher shear-rates. In general, the contact duration increases with both shear-rate and concentration with a good number of contacts lasting much longer than the binary contact time. Furthermore, the effect of concentration on these contact times is evident from these results. Log-normal distribution seems to fit the lower concentration case ($C=0.8$) well, but not for higher concentrations. Figure 12 depicts the mean contact duration for both frictionless and frictional cases and various dimensionless shear-rates and concentrations. All cases show that the mean contact duration is longer than the duration of binary collision. The frictional cases have much longer contact time than the corresponding frictionless cases. An interesting result is that as shear-rate increases the mean contact duration begins to decrease. It is probably due to the degradation of the group stability sustaining the multiple collisions under high shear-rates.

V. DISCUSSION

The data obtained from the numerical experiment support the conceptual theory given in Sec. III. As shown in Figs. 6–8, we observe at lower shear-rates and lower concentrations, the particles are mostly discrete and the contacts are rare. A significant portion of the contacts are binary in nature (as seen from the group size values in Fig. 7). Hence as the shear-rate increases, the kinetic energy and the stress in-

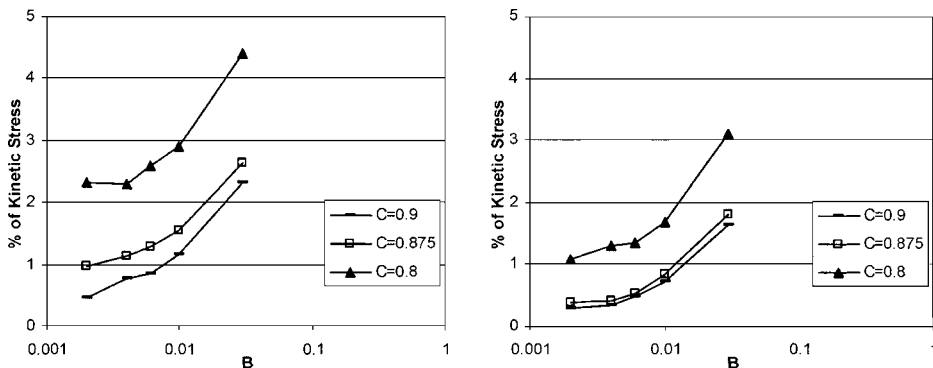


FIG. 10. Percentile of dimensionless kinetic stress τ_{22}^k/τ_{22}^* . Left side: $\mu=0$; right side: $\mu=0.5$.

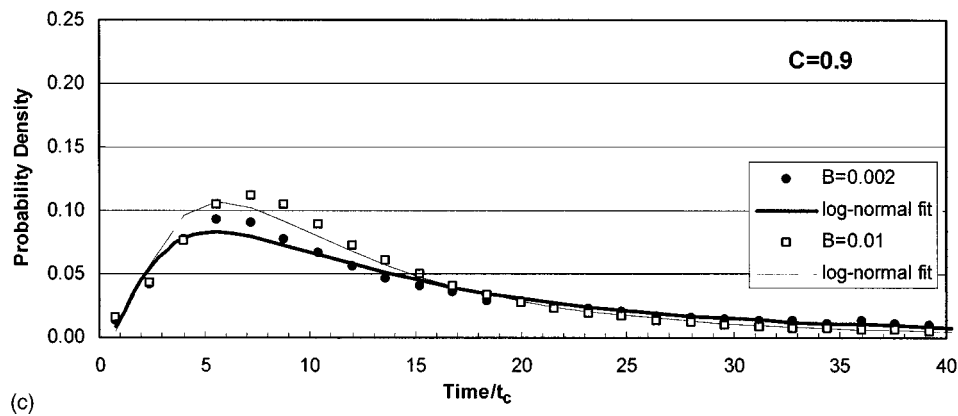
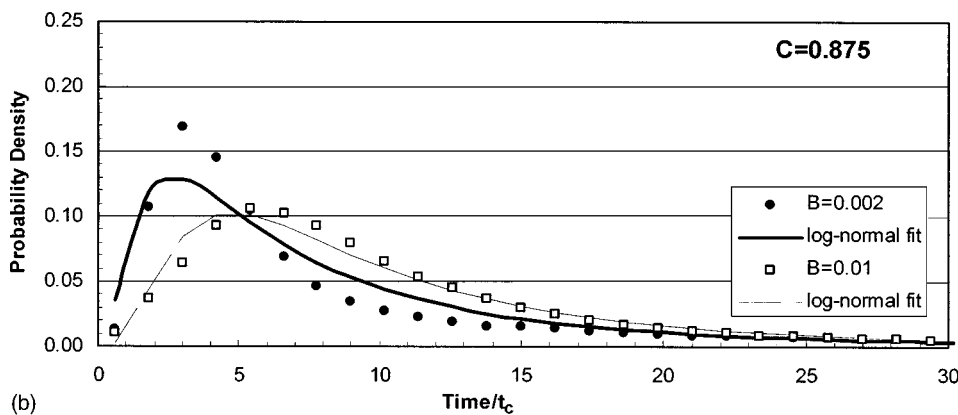
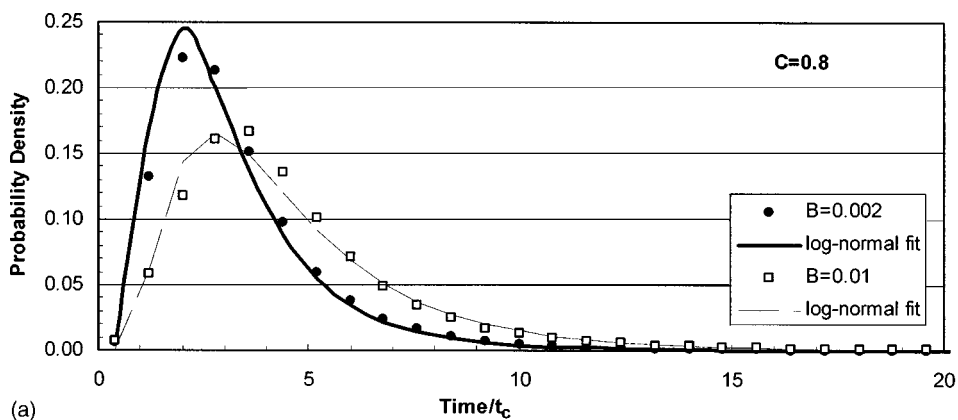


FIG. 11. Contact time distributions for $\mu=0$ and (a) $C=0.8$, (b) $C=0.875$, and (c) $C=0.9$.

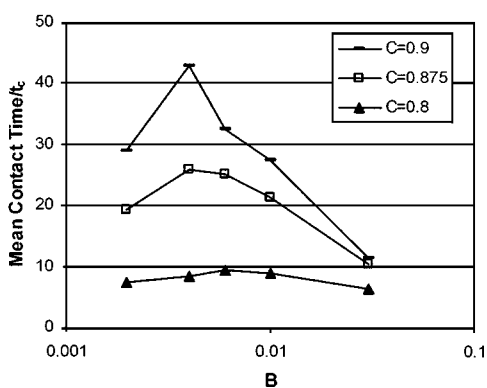
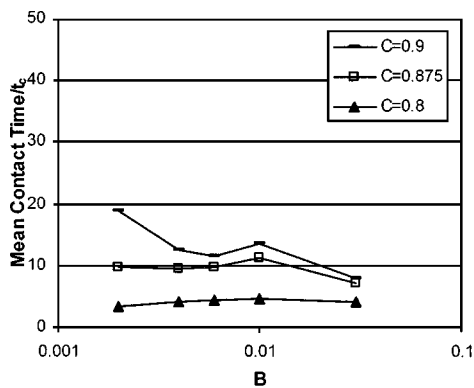


FIG. 12. Mean contact duration for various concentration and dimensionless shear-rates. Left side: $\mu=0$; right side: $\mu=0.5$.

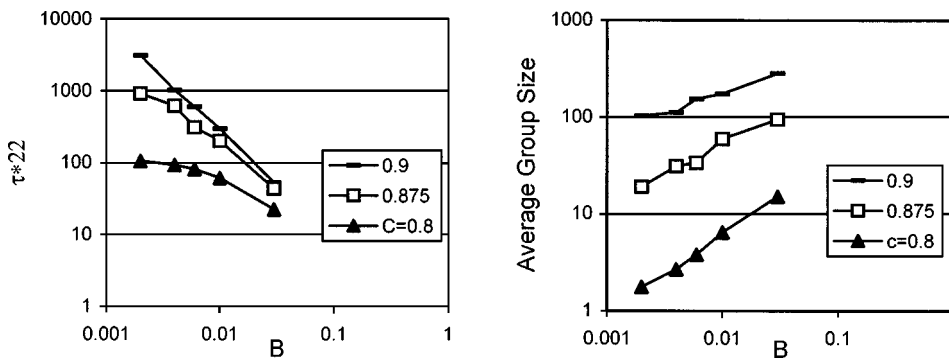


FIG. 13. Dimensionless normal stress and average group size for $e=0.9$, $\mu=0$ with all other parameters the same as in Figs. 6 and 7.

crease as the collisions become more frequent. At first, this increase of stress indeed is dependent on the square of the shear-rate, as shown by the flat curve in Fig. 5 for low shear-rate cases. If the shear-rate is increased for a lower concentration case ($C=0.8$), multiple collisions begin to take place, group size increases, rate dependency begins to drop as can be seen from the declining slope of the dimensionless stress curve in Fig. 6. For higher concentrations, such declining slope happens at lower shear-rates. Rate dependency of the constitutive relation does not totally disappear for $C=0.8$ in the range of B tested, suggesting groups of colliding particles may form and separate at a rate corresponding to the shear-rate. This point has also been mentioned in [18]. We believe the above results correspond to the inertial-collisional, inertial-noncollisional, and finally elastic-inertial transition as defined in [10]. The strict quasistatic case with no rate-dependency is not observed in this study. It is speculated that for strict rate-independency to happen, group size needs to reach the sample size consistently.

The integrity of the groups is related to the velocity fluctuation of the particles. As shown in Fig. 10, kinetic stress of the granular system does increase with shear-rate and decrease with solid concentration, indicating the dynamics of groups play a role in the constitutive relation of the granular material. The dynamics of group interactions are responsible for the rate dependency of the constitutive behavior even though binary collisions are no longer valid.

The constitutive relation of granular flows changes regimes from being rate-dependent to nearly rate-independent. This regime change may be explained in terms of the contact time also. From Fig. 11 the peak probability of contact time will occur around the binary contact time (time/ $t_c=1$) only for low concentration and low shear-rates. As either the shear-rate or the solid concentration increases, groups of particles form. The contact duration distribution peak is still distinct but the tail portion grows. Many more collisions are longer than binary, involving groups of simultaneously colliding particles. When shear-rate or solid concentration further increase, the force chain formation starts wherein the probability curve is sufficiently flat and the tail portion grows wider. Eventually, force chains become persistent wherein the probability curve could become flat across the entire time domain.

To see if any of the phenomena observed above is material property dependent, a case with $e=0.9$, $\mu=0$ was tested keeping all other parameters the same. The resulting dimensionless normal stress and the average group size are given in

Fig. 13. Similar behavior of all other parameters given in Figs. 8–12 was observed between $e=0.1$ and $e=0.9$. Nevertheless, it is with no doubt that regime change and the types of regimes depend quantitatively on the intrinsic properties at the grain level.

Granular materials are like any complex material that can display the whole range of behavior from solid to gas [29]. The gaslike extreme is the simplest form it can take. Transition between regimes seems to be related to evolutions of both additional time and length scales beyond the binary collision time and the individual particle size. It is observed that the contact time and the size of a group defined as the interconnecting particles both grow rapidly with increasing concentration while their dependence on the shear-rate is not monotonic.

Some additional remarks are due here concerning the very dense flows where force chains span the entire flow domain prevail. As mentioned in Ref. [10], interparticle friction plays an increasingly important role in very dense flows because the stability of these force chains rely on this friction. In the “elastic-quasistatic” regime stresses are mainly originated from the force chains. Increasing interparticle friction means more stable force chains and reduced inertia effects from their breakage. The resulting macroscopic behavior obeys a Coulomb friction law. The data from Ref. [10] suggested a percolation threshold exists for the solid concentration, above which rate-independency is expected.

All of the observations above are obtained from computer simulations. Since computer simulations are constrained by finite sample size, it is natural to ask whether the above observations are sample size dependent. We tested the stress and strain rate relations with sample size ranging from 20 by 20 to 50 by 50 and found quantitatively the results did depend on the sample size for small sample sizes. However, the stress results from 50 by 50 sample size are less than 5% of difference from the stress results of 30 by 100 presented here. Thus the stress and strain rate relations with the current sample size have probably reached its stable value for the parameters we tested. On the other hand, it is obvious that other internal scales may still be sample size dependent. For instance, when the maximum group size shown in Fig. 8 reaches the sample size, the mean and maximum group sizes are artificially constrained by the sample size. Thus although the qualitative behavior of granular flows, and reasons of the transition between distinct regimes is the same regardless of sample sizes, quantitative results reported in the above may still vary with sample size. Further study is required to address this issue.

VI. CONCLUSION

The results obtained in this paper show that the regime change for granular flows is related to additional internal length and time scales. Using a numerical experiment, the development of these additional scales is demonstrated by measuring the collision duration of the particles, the coordination number, and the size of the groups of simultaneously contacting particles. Although the results support the conceptual theory for regime change, it requires further analysis to determine how the particle groups interact and how the force chains form and break within these groups. These macroparticles are integral parts of a mathematical formulation of granular flows. The dynamics of these structures must be included in the constitutive laws for granular materials.

ACKNOWLEDGMENTS

We thank Jim Jenkins, Dan Hanes, and Dmitry Garagash for stimulating discussions, and Shunying Ji for independently verifying all numerical results. This study is supported by NASA Microgravity Fluid Physics Program grant number NAG3-2717.

APPENDIX

The notation used in this paper is as follows: B , dimensionless shear-rate; C , concentration; dt step size in the simulation= $t_c/50$; e , restitution coefficient; K_n, K_t , particle stiffness; m , particle mass; t_c , binary collision; $\dot{\gamma}$, shear-rate; μ , particle friction coefficient; τ_{22}^* , dimensionless normal stress; τ_{12}^* , dimensionless shearing stress.

-
- [1] J.T. Jenkins and S.B. Savage, *J. Fluid Mech.* **130**, 187 (1983).
 [2] C.S. Campbell, *Annu. Rev. Fluid Mech.* **22**, 57 (1990).
 [3] M.A. Hopkins and M.Y. Louge, *Phys. Fluids A* **3**, 47 (1991).
 [4] O.R. Walton, H. Kim, and A.D. Rosato, *Mechanics Computing in 1990's and Beyond*, edited by H. Adeli and R. L. Sierakowski, ASCE Engineering Mechanics Specialty Conference Monograph (American Society of Civil Engineers, New York, 1991), p. 1249.
 [5] S. Luding and H. J. Herrmann, *Chaos* **9**, 673 (1999).
 [6] B. Painter, M. Dutt, and R.P. Behringer, *Physica D* **2979**, 1 (2002).
 [7] C.K.K. Lun, S.B. Savage, D.J. Jeffrey, and N. Chepurny, *J. Fluid Mech.* **140**, 223 (1984).
 [8] O.R. Walton and R.L. Braun, *J. Rheol.* **30**, 949 (1986).
 [9] M. Babic, H.H. Shen, and H.T. Shen, *J. Fluid Mech.* **219**, 81 (1990).
 [10] C.S. Campbell, *J. Fluid Mech.* **465**, 261 (2002).
 [11] S.B. Savage, in *Mech. Granular Materials: New Methods and Constitutive Relations*, edited by J.T. Jenkins and M. Satake (Elsevier, Amsterdam, 1983), p. 261.
 [12] P.C. Johnson and R. Jackson, *J. Fluid Mech.* **176**, 67 (1987).
 [13] P.C. Johnson, P. Nott, and R. Jackson, *J. Fluid Mech.* **210**, 501 (1990).
 [14] I. Goldhirsch, *Annu. Rev. Fluid Mech.* **35**, 267 (2003).
 [15] M. Oda, J. Konishi, and S. Nemat-Nasser, *Mech. Mater.* **1**, 269 (1982).
 [16] D.W. Howell, R.P. Behringer, and C.T. Veje, *Chaos* **9**, 559 (1999).
 [17] D.W. Howell, R.P. Behringer, and C.T. Veje, *Phys. Rev. Lett.* **82**, 5241 (1999).
 [18] D.Z. Zhang and R.M. Rauenzahn, *J. Rheol.* **44**, 1019 (2000).
 [19] E. Aharonov and D. Sparks, *Phys. Rev. E* **65**, 051302 (2002).
 [20] D. Volfson, L.S. Tsimring, and I.S. Aranson, *Phys. Rev. E* **68**, 021301 (2003).
 [21] S.B. Savage and M. Sayed, *J. Fluid Mech.* **142**, 391 (1984).
 [22] D.M. Hanes and D.L. Inman, *J. Fluid Mech.* **150**, 357 (1985).
 [23] T.G. Drake, *J. Geophys. Res., [Solid Earth Planets]* **95**, 8681 (1990).
 [24] C.S. Campbell, in *Powders & Grains 93*, edited by C. Thornton (A.A. Balkema, Rotterdam, the Netherlands, 1993), p. 289.
 [25] A.H. Cottrell, *The Mechanical Properties of Matter* (Wiley, New York, 1964), p. 201.
 [26] P. Thompson and G.S. Grest, *Phys. Rev. Lett.* **67**, 1751 (1991).
 [27] M.P. Allen and D.J. Tildesley, *Computer Simulation of Liquids* (Oxford University Press, New York, 1988).
 [28] R.C. Ball and R. Blumenfeld, *Philos. Trans. R. Soc. London, Ser. A* **360**, 731 (2003).
 [29] H.M. Jaeger, S.R. Nagel, and R.P. Behringer, *Rev. Mod. Phys.* **68**, 1259 (1996).